Strong Molecular Alignment Dependence of H_{2} Electron Impact Ionization Dynamics

X. Ren, T. Pflüger, S. Xu, J. Colgan, M. S. Pindzola, A. Senftleben, J. Ullrich, and A. Dorn

Phys. Rev. Lett. **109**, 123202 — Published 19 September 2012

DOI: 10.1103/PhysRevLett.109.123202

Strong molecular alignment dependence of H_2 electron impact ionization dynamics

X. Ren[1], T. Pflüger[2], S. Xu[3], J. Colgan[4], M.S. Pindzola[5], J. Ullrich[1,2] and A. Dorn[1]

[1] Max-Planck-Institute for Nuclear Physics, 69117 Heidelberg, Germany

[2] Physikalisch-Technische Bundesanstalt, Bundesallee 100, 38116 Braunschweig, Germany

[3] Institute of Modern Physics, Chinese Academy of Sciences, Lanzhou 730000, China

[4] Theoretical Division, Los Alamos National Laboratory, Los Alamos, New Mexico 87545, USA

[5] Department of Physics, Auburn University, Auburn, Alabama 36849, USA

Abstract

Low-energy (E_0 = 54 eV) electron impact single ionization of molecular hydrogen (H_2) has been investigated as a function of molecular alignment in order to benchmark recent theoretical predictions [Colgan et al., Phys. Rev. Lett. **101**, 233201 (2008) and Al-Hagan et al., Nature Physics **5**, 59 (2009)]. In contrast to any previous work we observe distinct alignment dependence of the (e, 2e) cross sections in the perpendicular plane in good overall agreement with results from time-dependent close coupling (TDCC) calculations. The cross section behavior can be consistently explained by re-scattering of the ejected electron in the molecular potential resulting in an effective focusing along the molecular axis.

PACS: 34.80.Gs, 34.80.Dp

The interaction of charged particles with matter is of fundamental importance in a broad range of sciences and applications. In quantum physics, inelastic scattering represents one of the most fundamental few-body problems. Much of our understanding of scattering processes through impact of charged particles has

emerged from kinematically complete studies in which the momentum vectors of all final-state particles are determined. Here, electron impact ionization, the so-called (e, 2e) reaction, is now considered to be well understood for the most simple systems such as atomic hydrogen and helium [1-3]. Much more challenging, however, is the treatment of atomic many-electron systems for which, e.g., non-perturbative theories are presently developed [4]. Even more demanding are multi-center targets like molecules [5, 6] or clusters [7]. Here, a range of new and interesting phenomena arise as a result of their increased complexity essentially due to additional degrees of freedom as compared to atoms. Examples are multiple scattering within the target itself, the interference of amplitudes for scattering at different centers, the exchange of angular momentum between the molecule and the continuum electrons or the non-isotropy of the ionized electron orbitals in the molecular-frame. In this context a large number of studies have been performed on H_2 which is the most simple and fundamental molecular system. Most of the previous (e, 2e) experiments were done under random orientation conditions, thus neglecting effects due to the molecular alignment (see e.g. [5, 6, 8-12]). As a result, versatile and important information on the collision dynamics is missing.

For the ionization of H_2 into its ionic excited states, (e, 2e) experiments with alignment determination were reported recently by Takahashi et al. to study the non-isotropic electronic structure of H_2 [13] as well as by Bellm et al. [14] to explore the collision dynamics for 174 eV electron impact. Ionization into the ionic ground state by 200 eV electron impact has been investigated by Senftleben et al. [15, 16]. However, all these investigations at relatively high impact energies essentially showed very little alignment dependence. In contrast, strong alignment dependence was predicted by time-dependent close coupling (TDCC) calculations for fully, fivefold differential cross section (FDCS) at lower impact energy and for electrons emitted perpendicular to the incoming projectile into the so-called perpendicular plane [17]. Respective experiments are missing so far due to low count rate in the perpendicular plane and exceptional challenges in fixing the molecular axis.

In this Letter we report on molecular-frame (e, 2e) cross sections for H_2 by

low-energy electron impact (E_0 = 54 eV). Strong alignment dependent effects are observed at a relatively large scattering angle ($\theta_{e1} = -50°$) and for emission of the second electron into the perpendicular plane. The energy sharing in the final state is varied from symmetric to asymmetric conditions and for molecular alignment determination, the ground-state dissociation (GSD) channel is exploited [15] where the residual H_2^+ ion dissociates into H^+ and H. GSD is almost identical to non-dissociative ionization since both processes involve the same initial and final electronic states with the only difference that GSD starts from smaller internuclear distances and populates dissociative vibrational wave functions of H_2.

The experiment was performed using a dedicated reaction microscope [18, 19]. Details about the molecular-frame (e,2e) experiment have been described elsewhere [16]. Briefly, a pulsed electron beam crosses a H_2 gas jet. Using uniform electric and magnetic fields the final state fragments, electrons and ions are projected (with almost 4π solid angle) onto two position- and time-sensitive multi-hit detectors. From the positions of the hits and the fragment times of flight, the momentum vectors of the detected particles can be calculated. Triple-coincidence detection of both outgoing electrons and the proton was achieved. The molecular alignment determination makes use of the detected proton momentum and is based on the axial recoil approximation [20].

Due to the extraordinarily small fraction of ground-state dissociating ionization in the order of 2%, the data accumulation time was of the order of 10 weeks. For a particular alignment angle the apex angle of the allowance cone was ±20°, corresponding in total to 6% of a spherical surface. The perpendicular plane geometry is selected by requesting that one electron is emitted within 90° ± 15° with respect to the incoming beam direction.

The time-dependent close-coupling method used here for comparison has been described in detail previously [21, 22]. Our calculation is made at a fixed internuclear separation which in this case is chosen to be R = 1.1 a.u., in order to precisely mimic the ground-state dissociation conditions [23].

In order to illustrate the chosen collision kinematics a three-dimensional (3D) polar plot of the measured non-dissociative ionization cross section is presented in Fig. 1 (a, b) for averaged alignment. The projectile ($\vec{p}_0$) is coming in from the bottom and scatters off the target in the origin of the coordinate system. One electron emission angle is fixed to $\theta_{e1} = -50°$ with respect to the projectile forward direction. The emission angle of the second electron is observed over the full 4π solid angle with equal energy sharing of the two outgoing electrons. The cross section pattern is governed by the well-known double-lobe structure: the binary lobe in the direction of momentum transfer $\vec{q}$ corresponds to electrons emitted in a single binary collision with the projectile. Its shift away from $\vec{q}$ to larger angles is due to post collision repulsion between the two outgoing electrons. The second, much smaller recoil lobe directed downward is attributed to a binary collision followed by backscattering in the ion potential resulting in emission roughly in the direction of $-\vec{q}$.

Here, we focus on the emission pattern perpendicular to the projectile indicated by grey shaded plane in Fig. 1(a). This region is magnified in (b). In panel (c) and (d) polar as well as Cartesian representations of the perpendicular pattern are shown for ground-state dissociation with averaged alignment. The cross section pattern reveals three individual peaks. One central very small peak at ϕ_{e2} close to 0° originating from the tail of the binary peak accompanied by two additional side lobes at $\phi_{e2} \approx \pm 60°$. Concerning TDCC theory, very good agreement in the relative shape of the cross section is obtained except a slight discrepancy with experiment close to $\phi_{e2} = \pm 180°$. The experimental non-absolute data are normalized to the TDCC calculation in the peak region. Thus, all the molecular-frame (e, 2e) data are normalized according to this scale.

In Fig. 2 FDCS are shown for molecular alignment along the x-, y- and z-spatial axis for the same kinematics as in Fig. 1 (c) and (d) ($\theta_{e1} = -50°$, $E_{1,2} = 18$ eV). The H_2 alignment is indicated by the blue spheres in the left column of Fig. 2 where polar plots of the data are presented while Cartesian plots of the same data are shown in the

right column. For cases where the molecular axis is within the detection plane its alignment is indicated by (blue) arrows. Since these scattering geometries show mirror symmetry with respect to the x-z plane, the experimental data were mirrored too with respect to ϕ_{e2} = 0°. Going through the diagrams, strong alignment dependence of the patterns is observed. Experimentally, for all cases we see a maximum along the positive x-axis as a remnant of the binary peak. For molecular alignment along the z-axis the angular emission pattern is broad, unstructured and quite similar to the non-aligned case. For x-alignment a narrower peak is observed along the alignment axis which is slightly increased in magnitude. Finally, for y-alignment three individual peaks occur, one along the x-axis and the side peaks roughly along the molecular axis. Taking these observations it appears in general as if the molecular potential redirects the emitted electrons resulting in effective focusing along the molecular axis. Such potential scattering effects should increase with decreasing electron energy. In Fig. 3 the electron energy is reduced from E_2= 18 eV in panel (a) to E_2= 10 eV in (b) and 4 eV in (c) for molecular alignment along y-axis. At 10 eV clearly the side lobes have increased and are of the same magnitude as the central peak. For 4 eV the side lobes become dominant and the central peak has decreased significantly in intensity resulting in an emission pattern strongly aligned along the molecular axis. This confirms the focusing influence of the molecular potential on the ejected electron pattern along the alignment axis.

In the following we present geometries where the symmetry with respect to the x-z plane is broken. In Fig. 4(a) the molecular axis starting from alignment along the x-axis is rotated by 45° around the z-axis. As result the cross section pattern shows a peak rotated in the same way. Interestingly, the asymmetry increases if the molecule is turned out of the perpendicular plane as it is shown in Fig. 4 (b). Here, the central peak intensity has decreased and the side lobe belonging to the molecular center pointing along the incoming projectile forward direction has increased in magnitude. For both cases emission along the opposite direction of the molecular axis could be assumed to be suppressed due to PCI effects. This is different when, starting from the

geometry in (b), the molecular axis is rotated by another 45° around the z-axis resulting in the molecular axis lying in the y-z plane [panels (c)]. The projection of the molecular axis into the observation plane (black dots) is aligned along the y-axis. Now electron emission along both directions ϕ_{e2} = -90° and +90° should experience identical PCI. Nevertheless, the emission pattern is strongly asymmetric and emission along the forward pointing proton projection (ϕ_{e2} = 90°) is clearly favored with respect to the opposite direction (ϕ_{e2} = -90°). The position of the side peak in the cross section pattern follows the molecular axis projection and shifts to larger ϕ_{e2} angles in going from (b) to (c). Finally, the asymmetry shrinks down as the forward pointing proton turns into the fixed electrons half plane by rotating the molecule by another 45° around the z-axis as it is shown in (d). Nevertheless, electron emission into the positive y-half plane and, thus, for positive ϕ_{e2} angles is still preferred compared to negative ones. In comparison with theory, the measured molecular-frame (e, 2e) patterns are rather well reproduced by the TDCC calculations. In Fig. 2 discrepancies are visible for alignment along the z-axis where experiment shows larger intensity at ϕ_{e2}= 0° and ±180°. For x-alignment the observed strong central peak is also present in theory albeit not as narrow as in the experiment. Good agreement is found for y-alignment (Fig. 3) where all three experimental peaks are reproduced except discrepancies in the magnitude of the central peak. In Fig. 4 theory reproduces a strong left/right asymmetry while there are discrepancies with experiment in the positions and intensities of the side lobes.

Overall, these observations are in strong contrast to previous experiments for ionization into the electronic ground state of H_2^+ with various projectiles where no alignment effects were observed. Among them are studies for photoionization at low emission energy [24-27], for ion impact [28] and our previous (e,2e) experiments at higher energy of 200 eV [15, 16]. The reason could be that the electrons in H_2 occupy binding orbitals smeared out over regions much larger than the internuclear distance showing only little anisotropy with respect to the molecular axis in position space as well as in momentum space [29].

For the present kinematics two aspects contribute to the visibility of alignment

dependence. On one hand we have chosen an observation plane where the cross section of the main lobes is small such that the relatively weaker alignment sensitive features become prominent. On the other hand, the alignment sensitivity in this plane can be motivated in a simple semi-classical picture: experimentally a large momentum of $\vec{q}$ = 1.54 a.u. is transferred to the target essentially in the forward direction (see $\vec{q}$ vector in Fig. 1). In a binary collision with the target electron this can be emitted into the perpendicular plane only if the longitudinal component of $\vec{q}$ is compensated by an equally large but opposite momentum in the initial bound state. The H_2 orbital shows such large momentum only in the high momentum tail of the Compton profile [29] which is the reason for the strongly reduced magnitude of the binary peak in the perpendicular plane. Classically these large momenta are present only close to the nuclei. If an electron is ejected from a region relatively close to a nucleus its trajectory should be sensitive to the position of the second nucleus and, therefore, to the alignment of the molecule.

In conclusion we have reported the first observation of distinct alignment dependence of molecular-frame (e, 2e) cross sections in the perpendicular plane. The observed features are rather well reproduced by TDCC theory. The FDCS patterns reveal that the positions and intensities of the side lobes and also the intensity of the central lobe strongly depend on the molecular alignment. According to their behavior, the side lobes arise from re-scattering of the outgoing electron in the molecular potential resulting in a focusing along the molecular axis.

In the present study interference effects which are regularly discussed for the scattering of H_2 by charged particle impact [11, 30] are not expected to show up due to the low kinetic energies which correspond to deBroglie wavelengths much larger than the internuclear separation. In future, for sufficient high impact energy the present experimental technique will enable unprecedented tests of existing interference observations which all were performed for non-aligned targets.

X.R. is grateful for support from DFG Project No. RE 2966/1-1. S.X. would like to

thank the support of the CAS-MPS doctor training program. The Los Alamos National Laboratory is operated by Los Alamos National Security, LLC for the NNSA of the U.S. DOE under Contract No. DE-AC5206NA25396. A portion of this work was supported by the US NSF and US DOE.

References

[1] T. N. Resigno, M. Baertschy, W.A. Isaacs, C.W. McCurdy, Science **286**, 2474 (1999).

[2] X. Ren, I. Bray, D.V. Fursa, J. Colgan, M.S. Pindzola, T. Pflüger, A. Senftleben, S. Xu, A. Dorn, and J. Ullrich, Phys. Rev. A **83**, 052711 (2011).

[3] O. Zatsarinny and K. Bartschat, Phys. Rev. Lett. **107,** 023203 (2011).

[4] O. Zatsarinny and K. Bartschat, Phys. Rev. A **85**, 032708 (2012).

[5] O. Al-Hagan, C. Kaiser, D. Madison, and A.J. Murray, Nature Physics **5**, 59 (2009).

[6] X. Ren, et al., Phys. Rev. A **82**, 032712 (2010).

[7] T. Pflüger, A. Senftleben, X. Ren, A.Dorn, and J. Ullrich, Phys. Rev. Lett. **107**, 223201 (2011)

[8] N. Lermer, B.R. Todd, N. M. Cann, Y. Zheng, C. E. Brion, Z. Yang, and E. R. Davidson, Phys. Rev. A **56**, 1393 (1997).

[9] M. Takahashi, Y. Khajuria and Y. Udagawa, Phys. Rev. A **68**, 042710 (2003).

[10] A. J. Murray, J. Phys. B **38**, 1999 (2005).

[11] D. S. Milne-Brownlie, M. Foster, J. Gao, B. Lohmann, and D. H. Madison, Phys. Rev. Lett. **96**, 233201 (2006).

[12] E. M. Staicu Cassagrande, et al., J. Phys. B **41**, 025204 (2008).

[13] M. Takahashi, N. Watanabe, Y. Khajuria, Y. Udagawa, and J. H. D. Eland, Phys. Rev. Lett. **94**, 213202 (2005).

[14] S. Bellm, J. Lower, E. Weigold, and D. W. Mueller, Phys. Rev. Lett. **104**, 023202 (2010).

[15] A. Senftleben, T. Pflüger, X. Ren, O. Al-Hagan, B. Najjari, D. Madison, A. Dorn, and J. Ullrich, J. Phys. B **43**, 081002 (2010).

[16] A. Senftleben, O. Al-Hagan, T. Pflüger, X. Ren, D. Madison, A. Dorn, and J. Ullrich, J. Chem. Phys. **133**, 044302 (2010).

[17] J. Colgan, M.S. Pindzola, F. Robicheaus, C. Kaiser, A.J. Murray, and D.H. Madison, Phys. Rev. Lett. **101**, 233201 (2008).

[18] J. Ullrich, R. Moshammer, A. Dorn, R. Dörner, L.Ph.H. Schmidt, and H. Schmidt-Böcking, Rep. Prog. Phys. **66**, 1463 (2003).

[19] M. Dürr, C. Dimopoulou, B. Najjari, A. Dorn and J. Ullrich, Phys. Rev. Lett. **96**, 243202 (2006).

[20] R.N. Zare, J. Chem. Phys. **47**, 204 (1967).

[21] M.S. Pindzola, F. Robicheaux, S. D. Loch and J. Colgan, Phys. Rev. A **73**, 052706 (2006).

[22] J. Colgan, O. Al-Hagan, D. H. Madison, C. Kaiser, A.J. Murray, and M.S. Pindzola, Phys. Rev. A **79**, 052704 (2009).

[23] A. Senftleben, T. Pflüger, X. Ren, B. Najjari, A. Dorn, and J. Ullrich, J. Phys. B **45**, 021001 (2012).

[24] J.H.D. Eland, M. Takahashi, and Y. Hikosaka, Faraday Discuss **115**, 119 (2000).

[25] A. Lafosse, M. Lebech, J. C. Brenot, P. M. Guyon, L. Spielberger, O. Jagutzki, J. C. Houver, and D. Dowek, J. Phys. B **36**, 4683 (2003).

[26] S.K. Semenov and N.A. Cherepkov, J. Phys. B **36**, 1409 (2003).

[27] J. Fernandez and F. Martin, New J. Phys. **11**, 043020 (2009).

[28] N. G. Johnson, R. N. Mello, M. E. Lundy, J. Kapplinger, E. Parke, K. D. Carnes, I. Ben-Itzhak, and E. Wells, Phys. Rev. A **72**, 052711 (2005).

[29] K.T. Lueng, and C.E. Brion, Chem. Phys. **82**, 113 (1983).

[30] N. Stolterfoht, et al., Phys. Rev. Lett. **87**, 023201 (2001).

Fig. 1

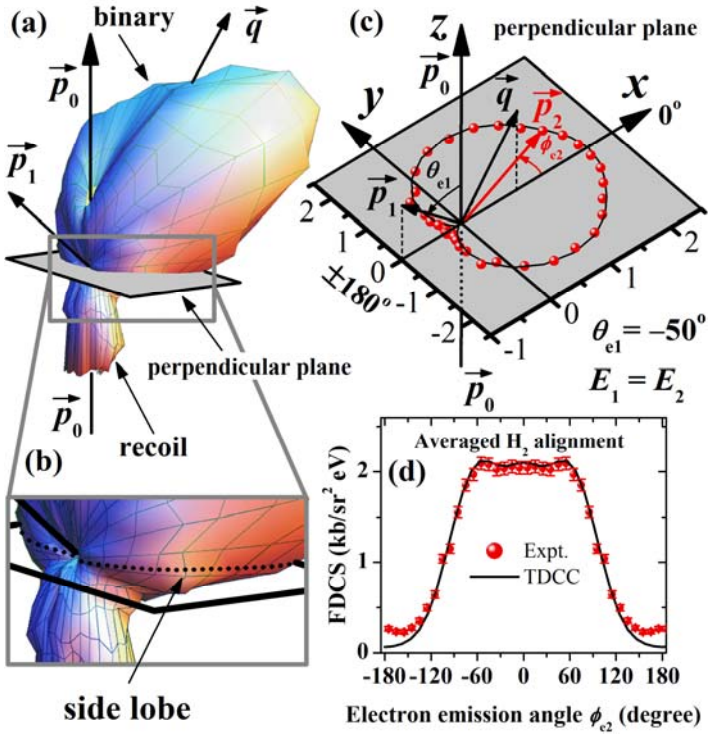

Figure 1 (Color online): Differential cross sections for the ionization of H_2 by 54 eV electron impact as a function of the emission angle of one electron with the other electron fixed to $\theta_{e1} = -50°$, equal energy sharing ($E_1 = E_2$) and averaged H_2 alignment. (a) Experimental 3D cross section for non-dissociative ionization and (b) the zoomed 3D cross section into the perpendicular region in (a). (c) and (d) are the electron emission patterns in the perpendicular plane for the dissociative ionization. Panel (c) displays the results in a polar plot while (d) shows the same data in a Cartesian representation.

Fig. 2

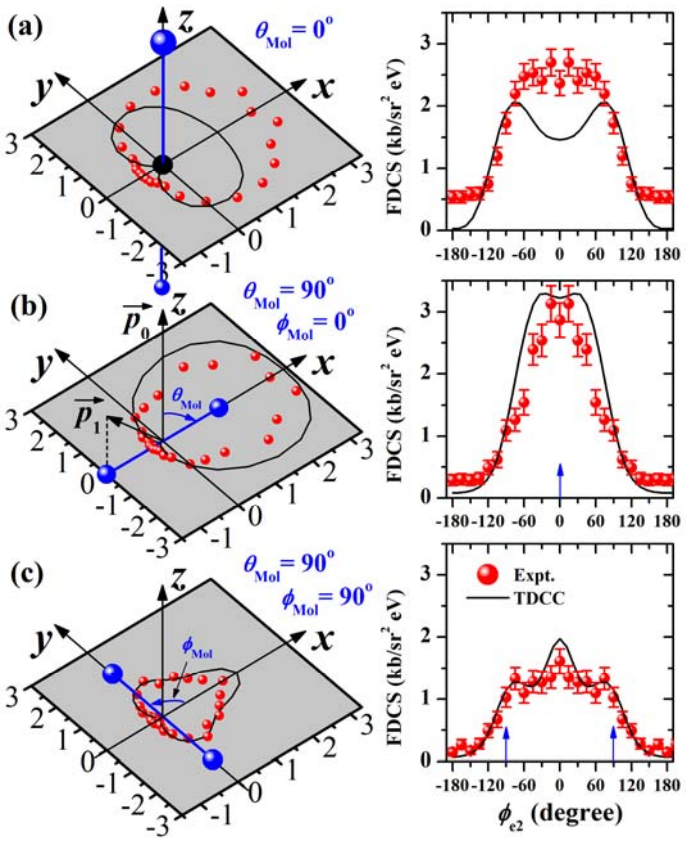

Figure 2 (Color online): Fully differential cross sections for the ionization of aligned H_2 molecules and equal energy sharing ($E_1 = E_2 = 18$ eV) with one electron emission angle fixed to $\theta_{e1} = -50°$ ($\vec{p}_1$ indicated in (b)) as a function of the emission angle of the second electron in the perpendicular (x-y) plane. The H_2 molecule is aligned as indicated by the blue spheres in the left column along the z-axis (a), the x-axis (b) and the y-axis (c). While the left column displays the FDCS in a polar plot, Cartesian plots are shown in the right column.

Fig. 3

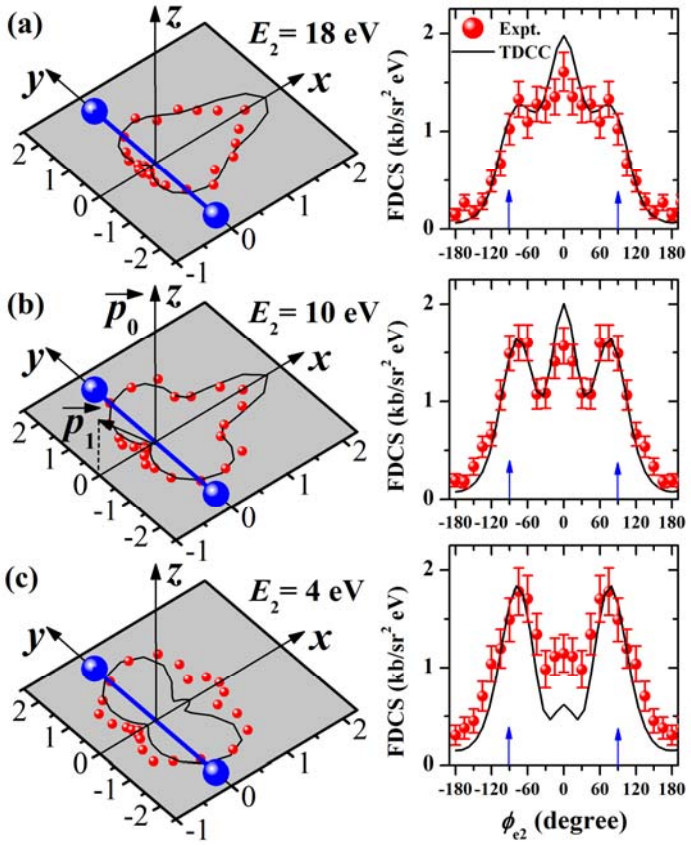

Figure 3 (Color online): As Figure 2 with the y-axis alignment (θ_{Mol} = 90°, ϕ_{Mol} = 90°) and variable energy sharing. From top to bottom row the electron energies are $E_1 = E_2$ = 18 eV (a), E_1 = 26 eV/E_2 = 10 eV (b) and E_1 =32 eV/E_2 = 4 eV (c).

Fig. 4

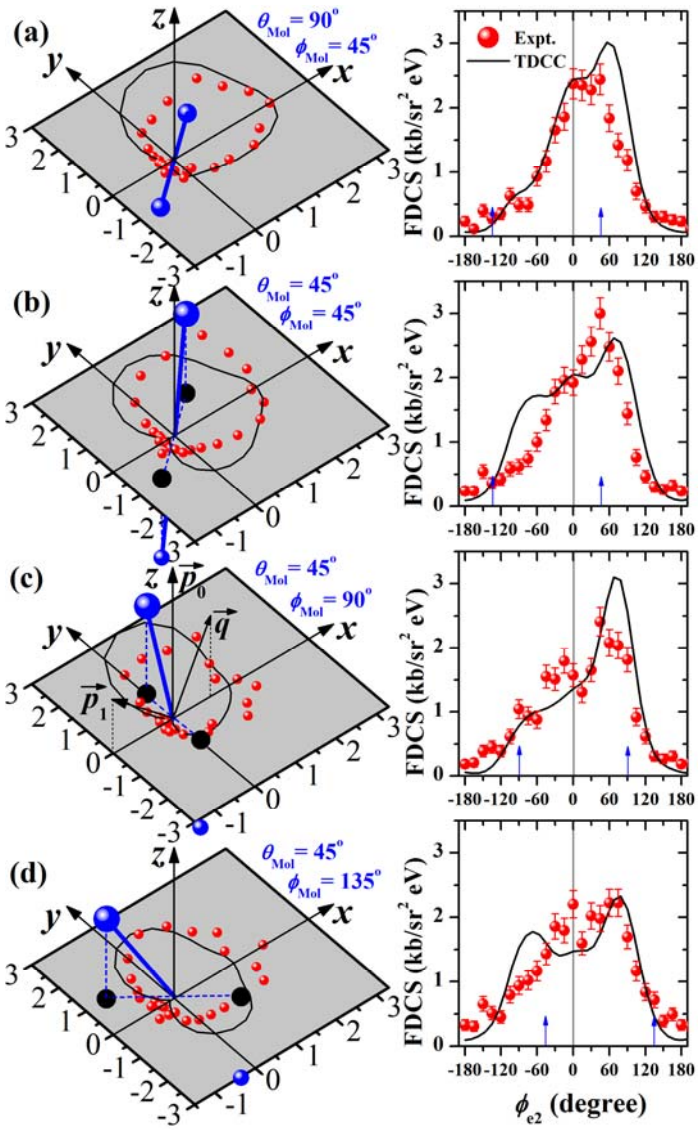

Figure 4 (Color online): As Figure 2 with H_2 alignment angles for which the reflection symmetry with respect to the x-z-plane is broken: (a) $\theta_{Mol} = 90°$, $\phi_{Mol} = 45°$; (b) $\theta_{Mol} = 45°$, $\phi_{Mol} = 45°$; (c) $\theta_{Mol} = 45°$, $\phi_{Mol} = 90°$; (d) $\theta_{Mol} = 45°$, $\phi_{Mol} = 135°$.